IMPLEMENTATION OF AN AUTOMATED ECG-BASED DIAGNOSIS ALGORITHM FOR A WIRELESS BODY SENSOR PLATFORM

Omitted for blind review

Keywords: Wireless Body Sensor Networks, Biomedical signal processing, Electrocardiogram

Abstract: Wireless Body Sensor Networks (WBSN) are poised to become a key enabling technology of personal systems for pervasive healthcare. Recent results have however shown that the conventional approach to their design, which consists in continuous wireless streaming of the sensed data to a central data collector, is unsustainable in terms of network lifetime and autonomy. Furthermore, it was established that wireless data communication is responsible for most of the energy consumption. To address the energy inefficiency of conventional WBSNs, we advocate an advanced WBSN concept where sensor nodes exploit their available, yet limited processing and storage resources to deploy advanced embedded intelligence and processing, to reduce the amount of wireless data communication and consequently energy consumption. More specifically, this paper addresses the design and optimization of an automated real-time electrocardiogram (ECG) signal analysis and cardiovascular arrhythmia diagnosis application for a prototype sensor node called *Wireless 25 EEG/ECG system*. The satifactory accuracy of this on-line automated ECG-based analysis and diagnosis system is assessed and compared to the salient off-line automated ECG analysis algorithms. More importantly, our results show an energy consumption reduction of 80% to 100% with respect to conventional WBSNs, when our analysis and diagnosis algorithm is used to process the sensed ECG data to extract its relevant features, which are then wirelessly reported to the WBSN central data collector, after the node can automatically determine the potential cardiovascular pathology without human monitoring.

1 INTRODUCTION AND RELATED WORK

Wearable personal health systems for pervasive monitoring and healthcare are widely recognized to be a key enabling integration technology for next-generation advanced citizen-centric eHealth delivery solutions (Lo and Yang, 2005). Through enabling continuous biomedical monitoring and care, they hold the promise of improved personalization and quality of care, increased ability of prevention and early diagnosis, and enhanced patient autonomy, mobility and safety. Furthermore, wearable personal health systems can help the eHealth sector realize its potentials in terms of rapid sustained market growth, reduction of healthcare costs and avoidance of unnecessary cost to the public purse.

To provide the necessary accurate, integrated and long-term assessment and feedback, these wearable personal health systems must sense, acquire, monitor and analyze a large number of physiological and metabolic parameters, both during physical activity and rest. The number as well as the nature of the parameters of interest depends on the actual biomedical application/scenario and target population. Nevertheless, it is largely accepted that Wireless Body Sensor Networks (WBSN) will be the underlying common architecture and technology of these personal health systems. More specifically, the WBSN will consist of a number of sensor nodes attached to the patient body, each sensor node potentially comprising of 5 components (Lazzer et al., 2002; Culler et al., 2004): sensors, actuators, a microprocessor, a wireless transceiver and an energy source. Each WBSN node ensures the accurate sensing and capture of its target physiological data, its (pre-) processing and wireless communication to the other nodes and the wearable Personal Digital Assistant (PDA). This PDA will be responsible for the storage, organization, complementary analysis and fusion of the collected information, its user-friendly representation, and its dissemination to the relevant medical staff or cen-

tral monitoring service through private and/or public wireless access networks (Lo and Yang, 2005).

State-of-the-art commercial products and experimental prototypes of personal health monitoring systems merely apply on-board analog filtering to the sampled sensed data, before it is either logged on a bulky patient unit for off-line analysis, or wirelessly transmitted to a remote monitoring system (Jovanov et al., 2005; LifeShirt; SmartShirt). The obtrusiveness and off-line nature of the analysis of the first approach compromises its acceptance and applicability to pervasive healthcare, whereas the second approach is not sustainable in free-living conditions in terms of autonomy. Indeed, current results in WBSN, e.g., prosthesis processing (Kemere et al., 2004) or Electroencephalogram (EEG) / Electrocardiogram (ECG) monitoring (Löfgren et al., 2007)) indicate that an unaffordable amount of energy would be spent in the wireless communication, if no local signal processing is present and most of the acquired data is wirelessly streamed to the PDA. Moreover, similar conclusions can be derived from the CodeBlue project (Project CodeBlue), which is a WBSN that targets biomedical monitoring by including a set of devices to collect ECG and oxigen saturation data, which can be transmitted through a wireless network to a wide range of receiving devices that can display the data in real time. The conclusions of this project outline that the largest proportion of energy is consumed in the wireless data transmission, and requires monitoring of the received data by a doctor or biomedical specialist; thus, the WBSN nodes are not able to report any physical anomaly. Therefore, we advocate in this paper an advanced WBSN concept where sensor nodes exploit their available processing and storage resources to deploy advanced embedded intelligence and processing, which will be optimized for enhanced functionality and autonomy. More particularly, in this paper, we investigate the feasibility and benefits of such an advanced WBSN for an automated electrocardiogram (ECG) signal analysis and cardiovascular arrhythmia recognition application, using a prototype sensor node called *Wireless 25 EEG/ECG system* (Omitted for blind review).

A significant amount of research effort has been devoted to the automated analysis of ECG signals, and the underlying detection of the major ECG characteristic waves, namely the QRS complex, P and T waves (Sörnmo and Laguna, 2005). As a matter of fact, the performance of an automated ECG analysis system critically depends on the reliable detection of these fiducial waves. The most salient methods proposed for the automated detection of the ECG fiducial waves belong to three categories: *filtering or adaptive thresholding*, *wavelet transform-based* and *(nonlinear) multiscale transform-based* (Sörnmo and Laguna, 2005). The latter approach was evidenced to have less noise sensitivity than adaptive thresholding, and to avoid the problem of position deviation exhibited by wavelet-based techniques. Therefore, in this paper, we consider a multiscale morphological derivative (MMD) transform-based algorithm to realize automated ECG characteristic wave detection.

While the retained MMD transform-based algorithm was validated by simulation (Sun et al., 2005), its translation into a robust, efficient and reliable automated diagnosis capability embedded in our wearable sensor node calls for the porting and (non-straightforward) optimization of this algorithm to adapt it to the sensor node's limited processing resources. In general, this porting and optimization effort is key to translate the recent biomedical signal processing advances into autodiagnosis tools, and hence to enable pervasive healthcare. As a result, the main contributions of the paper are the following ones:

- The design of a real-time ECG-based diagnosis algorithm, including a new run-time ECG signal reconstruction module, based on the off-line MMD algorithm, and a diagnosis module able to identify various anomalies in the cardiovascular function.
- The porting and sensible optimization of the new real-time ECG-based diagnosis algorithm on the Wireless 25-channel EEG/ECG sensor node platform.
- The application of the new diagnosis algorithm for autodiagnosis on-board the sensor node to significantly reduce the amount of data to be wireless transmitted, and consequently, dramatically reduce the sensor node's energy consumption and extend its battery life.

The rest of the paper is organized as follows. In Section 2, we overview the software and hardware architecture of the WBSN node used in this work. Then, in Section 3 we present the ECG-based diagnosis algorithm ported to our WBSN node. Next, in Section 4 we describe the performance and energy consumption trade-offs that have been identified between node processing and communication tasks. Finally, in Section 5, we summarize the main conclusions of this work.

2 WIRELESS BODY SENSOR NODE ARCHITECTURE

As previously mentioned, this work uses as target platform a Wireless 25-channel EEG/ECG sensor node (Omitted for blind review). This small sensor node can monitor up to 25 different bio-potential signals and transmit in real-time wirelessly the sensed information to a data collector device. Furthermore, it can be combined with other instances of the same

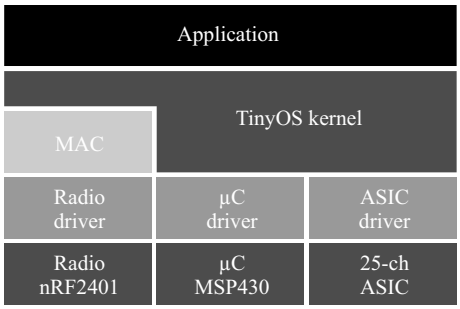

Figure 1: OS-Based EEG/ECG 25-ch sensor node architecture overview.

node to define complex WBSN topologies. The node has a very elaborated hardware/software architecture, which enables porting different types of biomedical signal processing applications, use different hardware components, and customize the communication stack for various wireless communication protocols. In this section we summarize the main features of the harware/software architecture of this node.

2.1 Hardware Architecture

The hardware architecture of the Wireless 25-channel EEG/ECG sensor node is partitioned in three main blocks, which relate to the three main tasks in WSNs, namely, sensing, processing and wireless transmission of the acquired information to a base station (e.g., a PC, PDA or a mobile phone).

The sensing task is performed by a 25-channel ultra-low-power Application-Specific Integrated Circuit (ASIC) that is able to extract the bio-potential signals. The core of the processing part is a TI MSP430 ultra-low-power microcontroller (Lutz Bierl, 2000). This small 16-bit microcontroller has a low active power (0.6 nJ/instruction), as well as a a very low stand-by power (2μW). In addition, it features a fast wakeup from stand-by to active mode (6μs) and an on-chip 12-bit analog-to-digital converter, suitable for biomedical signal processing. Finally, it also includes 60kB of flash program memory and 2kB of RAM to upload applications and store processed data from the different sensors.

Then, the wireless communication task is carried out using a Nordic nRF2401 transceiver (Nordic Semiconductor, 2000), which is an ultra-low-power 2.4 GHz communication chip. This component has a very low power consumption, with only 10.5mA at an output power of -5dBm and 18mA in receive mode. Also, it includes built-in power-down modes that allow to switch-off the radio when not used, and special transmission modes to reduce the processing needed by the microcontroller for every new packet sent or received. Overall, this radio is a very good low-power solution for WBSN that do not have very high duty cycle rates.

2.2 Software Architecture

The software architecture of the platform follows a layered modular approach in which each hardware component (sensors, microcontroller and radio) is a separate software module. This modular multi-layer structure, depicted in Figure 1, is supported thanks to the inclusion of TinyOS (Culler, 2006), a light event-based operating system specially designed for WSNs. It has been written using the nesC (Gay et al., 2003) programming language, which is an extension of the C language optimized for the memory restrictions of sensor networks. Thus, it is possible to easily port new biomedical signal processing applications using the nesC language, and to use the underlying hardware driver support provided by TinyOS to access different hardware blocks in the architecture. In addition, the abstraction from the hardware blocks makes possible to modify/replace the hardware blocks included in each instance of the node, without modifying the remaining blocks or the upper layers (communication protocols, applications, etc.). In particular, in this research work, while a porting for the TI MSP430 microcontroller was already available within the TinyOS hardware support, we had to develop the new drivers to support the Nordic nRF2401 radio module and the 25-channel EEG/ECG ASIC in the operating system, to be able to use them from the ECG-based diagnosis application layer.

3 ECG-BASED DIAGNOSIS ALGORITHM

The design of an ECG-based diagnosis algorithm to detect possible cardiovascular diseases is a very complex process that can be divided in two main phases. First, a real-time detection of the characteristic waves of ECG signals (Sun et al., 2005; Sun et al., 2002) (e.g., complex QRS, P and T wave, etc.) is an essential module for the quality of the detection of the cardiovascular diseases; thus, we have developed a run-time ECG wave identification module, which is described in Section 3.1. Second, once the fundamental features of the input ECG signal are identified, they can be used to detect if the heart is suffering an anomalous behavior of the cardiovascular function and diagnose corresponding pathologies. This last phase of the proposed ECG-based diagnosis algorithm is described in Section 3.2.

3.1 Run-Time ECG signal reconstruction

Our run-time ECG signal reconstruction phase is based on a multiscale morphological derivative

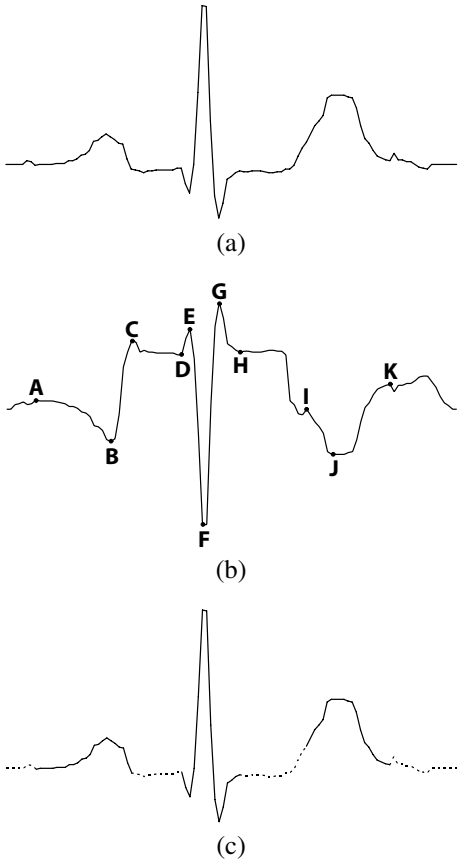

Figure 2: Results obtained using the MMD detector.
(a) Original ECG input signal (b) Multiscale morphological transform of the original signal (c) Points and waves detected by the algorithm
A=onset of the P wave, B=P peak, C=offset of the P wave, D=onset of the Q wave, E=onset of the R wave, F=R peak, G=offset of the R wave, H=offset of the S peak, I=onset of the T wave, J=T peak, K=offset of the T wave.

(MMD) transform-based singularity detector (Sun et al., 2005). This initial detector is an off-line algorithm able to reliably identify the Q wave, R peak, S wave and the onsets and offsets of the P wave and T wave, which are fundamental blocks of any ECG signal, as shown in Figure 2.

Although the ECG signal reconstruction using the MMD algorithm is quite accurate (Sun et al., 2005), the fundamental issue to directly apply for WBSN is the fact that MMD requires as input data the complete wave read from a patient during a large amount of time, which is subsequently processed to tune the thresholds to apply for each concrete sample. Unfortunately, the memory resources of a WBSN sensor node are very limited (only few kilobytes) to minimize its size and power consumption; thus, taking into account the high sampling frequency needed for a reliable ECG signal processing, only a few seconds of information can be stored, which is insufficient to accurately tune the thresholds for MMD. Moreover, if all the data is streamed from the sensor node to a device with larger capacity (e.g., a base station) to process them, the sensor node would run out of battery in a short period of time, because of the elevated data transmission rate that is needed and the high energy consumption of the radio. As a result, WBSN require an on-line approach for ECG signal reconstruction, in which the complete ECG signal is processed directly in the sensor nodes and only the relevant results are sent to the data collector device or base station.

1. The thresholds Th_r and Th_f are selected based on an adaptive thresholding from the histogram of the transformed signal
2. r_{peak} = local minima with absolute amplitude larger than Th_r
   If r_{peak} was not detected, go to 1, otherwise continue
3. r_{on} = first local maxima on the left of r_{peak} with absolute amplitude larger than Th_f
   r_{off} = first local maxima on the right of r_{peak} with absolute amplitude larger than Th_f
4. q_{wave} = first local minima on the left of r_{on} with absolute amplitude larger than Th_f
5. s_{wave} = first local minima on the right of r_{off} with absolute amplitude larger than Th_f
6. p_{off} = first local maxima on the left of q_{wave} with absolute amplitude larger than Th_f
   p_{on} = first local maxima on the left of p_{off} with absolute amplitude larger than Th_f
7. t_{on} = first local maxima on the right of s_{wave} with absolute amplitude larger than Th_f
   t_{off} = first local maxima on the right of t_{on} with absolute amplitude larger than Th_f

Table 1: Steps followed by the proposed run-time ECG signal reconstruction algorithm. All the operations are performed over the transformed data.

In the following we propose a run-time processing of the ECG signal, based on a MMD transform-based singularity detector, which can be directly executed in a WBSN sensor node. In the first phase of our run-time ECG fiducial wave detection algoritm, the received input signal is filtered for noise reduction and baseline wander correction (Sörnmo and Laguna, 2005). To this end, we have implemented a morphological filter on the input signal (Sun et al., 2002), where at all instances of time during the execution, a window of the last 300 samples are stored in a circular buffer. Hence, since the sampling frequency of the 25-channel EEG/ECG node is 200Hz, the current implementation of the algorithm uses the last 1.5s of the input signal as history of processed signal.

Once each sample is filtered, the following step in an MMD detector requires the application of a multiscale morphological transform on the filtered data to compare different versions of the input signal in the following phases to detect the fiducial points in the original ECG signal. However, due to the scarce memory resources in the node, the transformed signal cannot be stored in the node; thus, the morphological

transform is dynamically recalculated when needed during the following steps of the run-time algorithm. Then, the local maxima and minima of the transformed signal can be selected, based on some characteristics of the morphological trasform and a dynamic thesholding, updated at run-time using a window of the last received samples. These detected local maxima and minima are then subsequently used to locate the characteristic points of the wave. In this regard, since the sampling frequency is 200Hz, the microcontroller only has 5ms between two consecutive samples to perform all the calculations on the data to find the local maxima and minima. As this time interval is too short to execute the complete detection of maxima and minima points, we have divided the algorithm into 7 phases, which are listed in Table 1. Each of these phases can be executed in the interval between two consecutive samples. Thus, when a new data is sampled, filtered and included in the circular buffer, one of the 7 phases is executed. For example, at the beginning of the process, when no R peak is yet present in the considered window, steps 1 and 2 are repeated continuously between data samples. Then, when a R peak is detected in step 2, steps 3 to 7 are applied in sequence, such that, each of them is used in the time slot between two consecutive samples. After the complete identification of the current input ECG wave is finished, the process restarts from step 1 for the next wave.

For illustration purposes, one of the results obtained using the proposed run-time ECG signal reconstruction algorithm in an input wave is depicted in Figure 2. This figure shows three different waves, the first one (or a) is the original ECG signal given as an input to the algorithm. The second wave (or b) is the original signal after applying the multiscale morphological transform, all the points detected by the algorithm are marked. The last one (or c) shows the detected waves and peaks over the original signal. This last wave illustrates where the Q wave, R peak, S wave and the onsets and offsets of the P wave and T wave are found using the proposed run-time algorithm.

3.2 Arrhythmia detection phase

After processing the original ECG signal and obtaining the fiducial points of the wave (Figure 2), our diagnosis module is applied to check if the signal presents any anomalous behavior, which may hint that the patient is suffering a cardiovascular pathology.

The diagnosis module checks iteratively five different conditions based in the points detected in the ECG signal, according to the valid ranges reported in (Schamroth, 1971; Pérez-Gómez, 1985), namely:

1. The time from D to H must be less or equal to 0.10s.

HBR	RR	QTc and normal limits
40	1.5	0.46 (0.41 - 0.51)
50	1.2	0.42 (0.38 - 0.46)
60	1	0.39 (0.35 - 0.43)
70	0.86	0.37 (0.33 - 0.41)
80	0.75	0.35 (0.32 - 0.39)
90	0.67	0.33 (0.30 - 0.36)
100	0.60	0.31 (0.28 - 0.34)
120	0.50	0.29 (0.26 - 0.32)
150	0.40	0.25 (0.23 - 0.28)
180	0.33	0.23 (0.21 - 0.25)
200	0.30	0.22 (0.20 - 0.24)

Table 2: Normal values of the QTc. HBR=Heart Beat Rate (per minute), RR=RR interval. Values in last two columns are in seconds.

2. The time interval from A to D must be in the range from 0.12s to 0.20s.

3. The amplitude of J must always be positive.

4. The time from D to F must not be longer than 0.03s.

5. The QT interval rule, which establishes a relation between the interval from D to K. This rule indicates the valid interval between the heart beat rate, and the last RR interval (i.e., the interval from the last R peak to the current one). To find the valid QT interval, Bazet's formula (1) is used to calculate the QT coefficient for an input signal (QTc) as shown in Equation 1. Then, the valid values of the QTc are reported in Table 2.

$$QTc = \frac{time\ interval\ from\ D\ to\ K}{\sqrt{previous\ RR\ interval}} \quad (1)$$

As a result, in the current version of our diagnosis algorithm, according to the results of checking these previous five conditions, the sensor node reports to the base station that the heart of the monitored patient can be suffering one of the pathologies listed in Table 3.

4 EXPERIMENTAL RESULTS

The complete proposed ECG-based diagnosis algorithm has been ported and optimized to be executed in the 25-channel EEC/ECG node. The statistics and energy values that are shown in the rest of the paper were obtained using the model of the 25-channel EEG/ECG system for PowerTOSSIM, which was validated in (Omitted for blind review), showing variations in the results of less than 4% between the simulation framework and the measurements of the final platform.

Problem	Possible pathology
Time from D to H longer than 0.10s (it could even reach 0.12s).	Block of the His bundle. Supraventricular rhythm with aberrant conduction. Abnormal conduction over accesory pathways. Ventricular rhythm or pacemaker rhythm.
The time interval from A to D is longer than 0.20s (long PR interval).	Disorder in the conduction between atriums and ventricles at the atrioventricular node level, His bundle (or its branches) or Purkinje system.
The time interval from A to D is shorter than 0.12s (short PR interval).	Presence of an anomalous accesory pathway that produces a faster conduction or the presence of a rhythm with origin in the atrioventricular union, in the left atrium or in the lower part of the right atrium. Generally, this anomaly is due to a ventricular preexcitation.
The amplitude of J is negative (T wave is negative).	Primary alterations of the repolarization phase (due to ischemia or myocardial infarction, subacute pericarditis or myocarditis). Secondary alterations of the repolarization phase (due to alterations of the ventricular repolarization).
The time from D to F is longer than 0.03s.	Delay in the ventricular activation time.
QT interval longer than the values specified in Table 2.	The ventricular repolarization has slowed down, which can be due to acquired or congenital causes. It is related to the appearance of arrhythmias.
QT interval shorter than the values specified in Table 2.	This problem is usually related to the use of some medicines, hypercalcemia or hyperpotassemia.

Table 3: Possible pathologies that can be detected by the diagnosis module.

4.1 Validation of the ECG-Based Diagnosis Algorithm

The accuracy of the algorithm running on the 25-channel EEG/ECG system was tested with several input signals taken from the QT database (Laguna et al., 1997). This database was specially created for evaluation of algorithms that detect waveform boundaries in ECG signals. It consist of 105 fifteen-minute excerpts of two-channel ECG recordings. It also contains a subset of beats (at least 30 in each recording) that has been manually annotated by cardiovascular analysis experts.

In our first set of experiments we have compared the performance of the proposed algorithm with MMD and other state-of-the-art ECG detection algorithms from the literature for detection of waveform boundaries in ECG signals: the original MMD off-line algorithm (Sun et al., 2005), an adaptive thresholding-based detector (TD) (Daskalov and Christov, 1999) and a wavelet transform-based detector (WD) (Li et al., 1995).

Technique	*Parameter*	P_{on}	P_{off}	QRS_{on}	QRS_{off}	T_{on}	T_{off}
Ours	$Se(\%)$	92.4	92.4	100	100	96.6	91.7
	$m(ms)$	1.4	14.9	-7.8	8.2	53.6	12.8
	$\sigma(ms)$	15.6	13.3	22.6	16.8	21.6	20.9
MMD	$Se(\%)$	97.2	94.8	100	100	99.8	99.6
	$m(ms)$	9.0	12.8	3.5	2.4	7.9	8.3
	$\sigma(ms)$	9.4	13.2	6.1	10.3	15.8	12.4
TD	$Se(\%)$	96.2	97.0	99.9	99.9	98.8	98.9
	$m(ms)$	10.3	-5.7	-7.3	-3.6	23.3	18.7
	$\sigma(ms)$	14.1	13.6	10.9	10.7	28.3	29.8
WD	$Se(\%)$	89.9	89.9	100	100	99.1	99.2
	$m(ms)$	13.0	5.4	4.5	0.8	-4.8	-8.9
	$\sigma(ms)$	12.7	11.9	7.7	8.7	13.5	18.8
CSE	$\sigma(ms)$	10.2	12.7	6.5	11.6	-	30.6

Table 4: Comparative results of our run-time ECG characteristic wave detection and other state-of-the-art ECG detection algorithms

We report three parameters in these comparisons, namely, their mean error (m), standard deviation (σ) and Sensitivity (Se). We have used these parameters because they give a complete overview of the overall behavior of each algorithm, as m shows how close the detection results using an algorithm are to the manually annotated results, σ represents the stability of the detection and Se (defined in 2) measures the detection sensitivity (where TP is the number of true detections and FN is the number of manual annotations that are not detected by the algorithm).

$$Se = \frac{TP}{TP+FN} \times 100 \quad (2)$$

Table 4 shows the results obtained from these comparisons and the accepted standard deviation tolerances given by the Common Standards for Electrocardiography (CSE) committee. As this table illustrates, the values of the mean error are quite low and can be compared to the values obtained with MMD, TD and WD. Only in the case of T_{on}, the mean error is very high, but this is not a problem, since T_{on} is not relevant for the cardiovascular pathologies targetted by the diagnosis module. Then, the comparisons between the proposed run-time ECG signal reconstruction algorithm and the MMD detector in terms of σ is very important, since the proposed algorithm is based on the original off-line MMD detector. As expected, the values of the standard deviation achieved by the MMD method with the complete signal analysis instead of the limited run-time history are better. More precisely, the reasons for the improvement in standard deviation obtained by the MMD methods are due to the following factors:

- The proposed run-time algorithm is optimized to work in real-time in a sensor node platform, that is equipped with a very simple microcontroller. Float point operations are very costly in terms of time for such a simple microcontroller, and they had to be converted into integer operations, with the resultant loss of precision in the filtering and the multiscale morphological transform operations.

- Dynamic thresholding based on the histogram of the signal in the new approach is more difficult than with the off-line approach, since only a small window of data (the last 1.5s of signal) is available to choose the correct thresholds. Sometimes this is also a source of errors in the detections.

However, it is very important the fact that results using the proposed run-time approach are not far from the original algorithm, especially considering that, in exchange of a bit of accuracy, it is possible to process the input data in real-time and the patient can be informed of a possible cardiac pathology in real-time. Therefore, the time to react and attend the patient in case a problem is minimal, and then the consequences of the problem and the probability of the appearance of a more serious pathology derivated from a late identification of the problem are greatly reduced.

4.2 Energy Features of Diagnosis Sensor Node Platform in WBSN

One of the main problems in WBSNs is energy consumption, mainly due to the high sampling frequency required by these applications. Sensors generate lots of data that need to be transmitted to the base station, fot that reason, the time that sensors can be in standby mode is shorter than in other kind of applications. In these networks, the nodes are attached to the body, therefore batteries must be very small, to allow the person to do a normal life. This small batteries have a short lifetime and after some time they need to be replaced. If the sensors are implanted in the body, the replacement of the batteries is not feasible. A possible alternative could be energy scanvengers, but in general, energy scavengers are not able to supply the node continuously, the average power generated by one of these devices is usually much lower than the average power consumed by the nodes. Normally, they are coupled to batteries and recharge them, extending their lifetime.

Analyzing the energy consumption of the different hardware blocks of a node using typical applications for WBSNs, we can extract that the main cause of energy waste is the transmission and reception of data via radio. The radio is responsible for between 70% and 90% of the total amount of energy consumed by the whole sensor node. Then, one of the main challenges in WBSNs is trying to reduce as much as possible the energy consumption of the node, therefore we need to minimize the energy consumed by the radio, since the radio is the main source of energy waste.

In this section we consider and analyze three different approaches: data streaming, the use of the proposed run-time ECG signal reconstruction algorithm and the complete embedded diagnosis system, coupling the diagnosis module introduced in 3.2 to the basic run-time ECG algorithm.

	Sedentary	Fit	Sportperson
At rest	70 - 90	60 - 80	40 - 60
Aerobic	110 - 130	120 - 140	140 - 160
Anaerobic	130 - 150	140 - 160	160 - 200

Table 5: Typical ranges of heart beat rate per minute at rest and practising aerobic and anaerobic exercise for different kind of adult people.

	Sedentary	Fit	Sportperson
At rest	91 - 93%	92 - 94%	94 - 96%
Aerobic	87 - 89%	86 - 88%	84 - 86%
Anaerobic	85 - 87%	84 - 86%	80 - 84%

Table 6: Energy savings in the radio due to transmission using the run-time ECG detector instead of doing data streaming.

First, we analyze the most basic application, that simply performs data streaming, which means that all the data read by the sensors is transmitted to the base station without any intermediatte operation. All the information will be processed off-line in the base station. In order to perform a reliable ECG streaming, a sampling frequency of about 200Hz is required. Taking into account that the packet payload is 18 bytes and the size of each sample is 12 bits, we can conclude that 1000 packets are sent in 60s.

Using the run-time ECG signal reconstruction algorithm previously described, the sampled data are preprocessed before being sent. In this way, a packet is sent only when a R peak is detected. The sent packet contains when the R peak has been detected, the position of the rest of detected points respect the R peak and the amplitude of P peak, R peak and T peak. The number of packets sent in 60s using this algorithm would be equal to the heart beat rate per minute. Typical values of heart beat rate per minute are shown in table 5. Table 6 shows the energy savings in the radio due to transmission of packets obtained with the use of the proposed algorithm. In order to verify this theoretical results, some experiments were run in the simulator. The results of one of these simulations is presented in figure 3. This plot shows that the energy consumption due to packet transmission in the case of the ECG streaming application is 50.30mJ in a simulation of 60 real seconds. If the run-time ECG algorithm is used, the energy consumption drops to 3.73mJ for an input signal of 76 heart beats per minute, which means a reduction of 92.6%, as it was predicted in table 6.

As previously mentioned, a diagnosis module has been implemented and successfully tested. This module evaluates, taking as input the points detected by the run-time ECG signal reconstruction algorithm, if the ECG signal of the patient is normal or it presents any anomalous behavior. When a problem is detected, a packet is sent, containint the code of the diagnosed pathology and the points of the wave where the pathology was detected. In the worst case, when

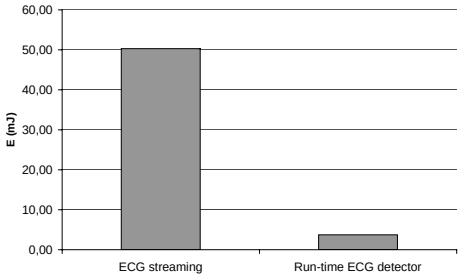

Figure 3: Energy consumption due to packet transmission for the ECG streaming application and the run-time ECG signal reconstruction algorithm during a period of 60s.

a problem is detected in every heart beat, the energy savings with regard to the data streaming case are the same as if we do not use the diagnosis module. In the best case, when no pathology is detected because the ECG signal is normal, no transmission is produced and therefore the reduction in the number of transmissions reaches 100% improvement.

5 CONCLUSIONS

Energy consumption minimization is one of the major design challenges to enable WBSN-based solutions for personal healthcare systems. In this paper, we have demonstrated the feasibility of exploiting the limited processing and storage resources to deploy a novel real-time automated ECG analysis and arrhythmia diagnosis algorithm on an actual sensor node platform. This goal was achieved through judicious application-level optimizations, taking into account the underlying hardware architecture and the real-time constraints of the automated diagnosis application. The satisfactory accuracy of both the automated ECG analysis (ECG characteristics wave detection) and ECG-based arrhythmia diagnosis algorithms was assessed. Finally, we also demonstrated that the deployment of these advanced algorithms for ECG analysis and autodiagnosis enables a dramatic reduction of the energy consumption (between 80% and 100%, depending on the sensed signal), compared to the conventional WBSN approach that simply wirelessly streams the sensed data to the central node. These excellent results show the potential of embedding advanced processing and intelligence in sensor nodes for extending the lifetime of WBSNs, and motivates further research in characterizing the optimal trade-off between embedded signal processing and wireless communications for these energy-constrained wireless networks.

REFERENCES

Culler, D. (2006). Tinyos: Operating system design for wireless sensor networks. *Sensors*, pages 41–49.

Culler, D., Estin, D., and Srivastava, M. (2004). Overview of sensor networks. *Computer*, pages 41–49.

Daskalov, I. K. and Christov, I. I. (1999). Automatic detection of the electrocardiogram T-wave end. *Med Biol Eng Comput*, 37(3):348–353.

Gay, D., Levis, P., von Behren, R., Welsh, M., Brewer, E., and Culler, D. (2003). The nesc language: A holistic approach to networked embedded systems. In *PLDI'03:Programming Language Design and Implementation*.

Jovanov, E. et al. (2005). A wban system for ambulatory monitoring of physical activity and health status: applications and challenges. In *International Conference of the IEEE Engineering in Medicine and Biology Society*.

Kemere, C. et al. (2004). Model-based decoding for reaching movement for prosthetic systems. In *International Conference of the IEEE Engineering in Medicine and Biology Society*.

Laguna, P., Mark, R. G., Goldberger, A. L., and Moody, G. B. (1997). A database for evaluation of algorithms for measurement of qt and other waveform intervals in the ecg. *Computers in Cardiology*, pages 673–676.

Lazzer, S., Feng, J., Koushanfar, F., and Potkonjak, M. (2002). System-architectures for sensor networks issues. In *IEEE International Conference on Computer Design (ICCD)*.

Li, C., Zheng, C., and Tai, C. F. (1995). Detection of ECG characteristic points using wavelet transforms. *IEEE Transactions on Biomedical Engineering*, 42:21–29.

LifeShirt. http://www.vivometrics.com.

Lo, B. and Yang, G. (2005). Key technical challenges and current implementations of body sensor networks. In *Second International Workshop on Wearable and Implantable Body Sensor Networks*.

Löfgren, N. et al. (2007). Eeg entropy estimation using a markov model of the eeg for sleep stage separation in human neonates. In *International Conference of the IEEE Engineering in Medicine and Biology Society*.

Lutz Bierl, Texas Instruments. (2000), MSP430 Family Mixed-Signal Microcontroller Application Reports. Technical Report TI-06-2000.

Nordic Semiconductor. (2000), nRF2401 Transceiver Data Sheets. http://www.nordicsemi.com/.

omitted for blind review.

Pérez-Gómez, F. (1985). *Cardiac Pacing*. Editorial Grouz.

Harvard University. Project CodeBlue. http://www.eecs.harvard.edu/ mdw/proj/codeblue/.

Schamroth, L. (1971). *The disorders od cardiac rhythm*. Blackwell Scientific Publications.

SmartShirt. http://www.sensatex.com.

Sörnmo, L. and Laguna, P. (2005). *Bioelectrical Signal Processing in Cardiac and Neurological Applications*. Elsevier Academic Press.

Sun, Y., Chan, K. L., and Krishnan, S. M. (2002). ECG signal conditioning by morphological filtering. *Computers in Biology and Medicine*, 32(6):465–479.

Sun, Y., Chan, K. L., and Krishnan, S. M. (2005). Characteristic wave detection in ecg signal using morphological transform. *BMC Cardiovascular Disorders*.